THE JOURNAL OF BIOLOGICAL CHEMISTRY VOL. 285, NO. 42, pp. 32303–32311, October 15, 2010

Probing the Conformation of a Prion Protein Fibril with Hydrogen Exchange*[S]

Received for publication, February 15, 2010, and in revised form, July 28, 2010 Published, JBC Papers in Press, August 2, 2010, DOI 10.1074/jbc.M110.114504

Steven M. Damo[‡1], Aaron H. Phillips[‡1], Anisa L. Young[§], Sheng Li[¶], Virgil L. Woods, Jr.[¶2], and David E. Wemmer[‡3]

From the Departments of [‡]Chemistry and [§]Molecular and Cellular Biology, University of California, Berkeley, California 94720 and the [¶]Department of Medicine and Biomedical Sciences Graduate Program, University of California San Diego School of Medicine, La Jolla, California 92093

A fragment of the prion protein, PrP(89–143, P101L), bearing a mutation implicated in familial prion disease, forms fibrils that have been shown to induce prion disease when injected intracerebrally into transgenic mice expressing full-length PrP containing the P101L mutation. In this study, we utilize amide hydrogen exchange measurements to probe the organization of the peptide in its fibrillar form. We determined the extent of hydrogen exchange first by tandem proteolysis, liquid chromatography, and mass spectrometry (HXMS) and then by exchange-quenched NMR. Although single amide resolution is afforded by NMR measurements, HXMS is well suited to the study of natural prions because it does not require labeling with NMR active isotopes. Thus, natural prions obtained from infected animals can be compared with model systems such as PrP(89–143, P101L) studied here. In our study, we find two segments of sequence that display a high level of protection from exchange, residues 102–109 and 117–136. In addition, there is a region that displays exchange behavior consistent with the presence of a conformationally heterogeneous turn. We discuss our data with respect to several structural models proposed for infectious PrP aggregates and highlight HXMS as one of the few techniques well suited to studying natural prions.

Prion diseases lead to neurodegenerative processes that result in spongiform degeneration and astrocytic gliosis in the central nervous system and are known to exist in genetic, sporadic and transmissible forms (1). The agent that is implicated in initiating disease is the protein PrP,[4] which can exist in two isoforms as follows: the benign native form PrP cellular and the infectious and neurotoxic form PrP^{Sc} (PrP scrapie) (2). Although non-protein factors, including nucleic acids and lipids, have been shown to facilitate the conversion from PrP cellular to PrP^{Sc} and modulate prion infectivity, it is clear that the PrP protein is required for prion passage (3–11). PrP is found in all mammalian and avian genomes and, after maturation, consists of approximately 200 residues with one disulfide bridge, two glycosylation sites, and is attached to the membrane via a C-terminal glycosylphosphatidylinositol anchor. Solution structures of PrP cellular, without post-translational modifications, from several organisms have been solved, showing it to be largely α-helical with an unstructured N terminus of approximately 100 residues (12–17). Experiments have shown that PrP binds copper and may be involved in copper homeostasis (18–20); however, the precise biochemical function of PrP remains unclear. For a detailed discussion, see the work by Aguzzi *et al.* (21). In contrast to the mostly α-helical, soluble PrP cellular, PrP^{Sc} is β-rich, with a protease-resistant core and is present as an aggregate (22). When PrP^{Sc} is proteolytically cleaved at its N terminus, it readily associates to form fibrils or rods that retain high levels of infectivity (23). Both electron microscopy and molecular mechanics calculations have been used to generate model structures for infectious PrP (24–27); however, due to their propensity to aggregate and the intrinsic insoluble nature, it has been difficult to obtain any high resolution structural information on infectious PrP with which a single model can be validated.

Determining the rates at which amide hydrogens exchange with solvent hydrogens provides a useful probe for hydrogen bonding in proteins. Exchange requires contact between the amide and solvent and catalysis by an acid or base (base dominates at neutral pH). Amides involved in hydrogen bonds thus cannot exchange without first fluctuating to an "open" state. Simple kinetic theories show that at neutral pH, the rates of exchange are determined by the equilibrium constant for opening and the intrinsic rate of exchange of the amide (determined by the identity of the amino acid and its sequence context) (28). Intrinsic exchange rates have been tabulated (29), so the observed exchange rates can be interpreted in terms of opening equilibria. At pH 7 and 25 °C, the intrinsic fully exposed amide hydrogen exchange rate is on the order of 10 s^{-1}. Recently, numerous groups have employed hydrogen exchange-based experiments to study amyloid fibrils formed from a number of different proteins, including PrP(89–230); note that throughout this study we use the mouse PrP numbering scheme (30–40). Interestingly, in each case it was shown that only subsets of

* This work was supported by the Army Prion Research Program Grant DMAD17-03-1-0476. Development of the HXMS methodology was supported by National Institutes of Health Grants AI076961, AI081982, AI2008031, AI072106, AI068730, GM037684, GM020501, and GM066170 (to V. L. W.), Innovative Technologies for the Molecular Analysis of Cancer Program Grants CA099835 and CA118595 (to V. L. W.), and Discovery Grant UC10591 from the University of California IUCRP Program, BiogenIDEC corporate sponsor (to V. L. W.).

[S] The on-line version of this article (available at http://www.jbc.org) contains supplemental Table S1, Fig. S1, and an additional reference.

[1] Both authors contributed equally to this work.

[2] To whom correspondence may be addressed. Tel.: 858-534-2180; Fax: 858-534-2606; E-mail: vwoods@ucsd.edu.

[3] To whom correspondence may be addressed. Tel.: 510-666-2683; Fax: 510-666-3384; E-mail: dewemmer@berkeley.edu.

[4] The abbreviations used are: PrP, prion protein; HXMS, tandem proteolysis, liquid chromatography and mass spectrometry; PrP^{C}, PrP cellular; PrP^{Sc}, PrP scrapie; GdnHCl, guanidine hydrochloride; HSQC, heteronuclear single quantum correlation; GSS, Gerstmann-Sträussler-Scheinker.

residues in the protein were protected from exchange with solvent, with rather different patterns of protected residues for different proteins. The remaining residues exhibited rapid exchange behavior characteristic of exposed amide groups.

One of the earliest animal models of prion disease was generated by expressing human PrP with a leucine substitution at P101L in transgenic mice at elevated levels; this mutation is implicated in Gerstmann-Sträussler-Scheinker disease (GSS), a familial form of prion disease. These mice developed sporadic GSS that could be serially passed to mice bearing the sensitizing mutation (41, 42). Later work reconstituted prion infectivity from a synthetic protein identified as a 55-residue PrP fragment, PrP(89–143, P101L), that readily associated into amyloid fibrils. Intracerebral injection of the aggregated fibrillar peptide initiated GSS in mice that express full-length PrP bearing the P101L mutation, whereas the nonaggregated peptide did not initiate disease (43). Furthermore, the peptide-initiated disease can be serially transmitted in mice bearing the same mutation (44).

Here, we describe amide hydrogen exchange behavior in the fibrillar form of PrP(89–143, P101L) obtained first at medium sequence resolution with tandem proteolysis, liquid chromatography, and mass spectrometry (HXMS) (45) and then at single amide resolution with NMR spectroscopy. We are able to observe regions of the peptide that are highly protected from exchange and others that are not. The strongly protected regions identify the residues in the hydrogen- bonded core of the amyloid fibrils of PrP(89–143, P101L).

EXPERIMENTAL PROCEDURES

Amyloid Fibril Formation—Amyloid fibrils of PrP(89–143, P101L) were formed by dissolving 10 mg of peptide into 500 μl of 20 mM sodium acetate, 100 mM NaCl, pH 5, and adding 500 μl of acetonitrile. Samples were taken at several time points, and EM images were collected. Small fibrils were seen even a short time after preparing the sample. At longer times primarily longer fibrils with more clearly defined edges were seen. Fibrils used in hydrogen exchange experiments were collected after 3 weeks of incubation in the acetonitrile solution. These fibrillization conditions are the same as used in previous bioassay experiments (43).

Electron Microscopy—Samples were loaded onto 1000 mesh copper grids, coated with Formvar, and glow discharged prior to use. The samples were negatively stained with 3% aqueous uranyl acetate, and images were collected on a FEI Tecnai 12 operating at 120 kV.

Hydrogen Exchange Mass Spectrometry—PrP(89–143, P101L)-peptide used in MS analysis was synthesized using standard Fmoc (*N*-(9-fluorenyl)methoxycarbonyl) chemistry and subsequent cleavage with trifluoroacetic acid. PrP(89–143, P101L) fibrils were collected by centrifugation at 1300 × *g* in an Eppendorf tube and washed twice with 10 mM sodium phosphate, pH 7.5. Deuterium exchange was initiated by resuspending the fibrils in 100% D_2O buffered with 10 mM sodium phosphate at a pH* of 7.5 (pH* is the reading of a pH meter, uncorrected for isotope and solvent effects) to a final peptide concentration of 50 mg/ml. 5-μl aliquots of the peptide suspension were removed after 1, 6, and 21 h and 1, 3, and 6 weeks. 5 μl of the peptide slurry was removed before exposure to deuterium to serve as the 0-h time point. Exchange samples were prepared for MS analysis by dilution with 55 μl of ice-cold 10 mM sodium phosphate buffer and rapid addition of 90 μl of quench buffer (6.8 M guanidine hydrochloride (GdnHCl), 16.6% glycerol, and 0.8% formic acid), yielding a final pH* of 2.1, followed by 5 min of incubation over thawing ice to fully dissolve the fibrils. Each solution was then divided into 50-μl aliquots in individual autosampler vials and rapidly frozen over powdered dry ice. Samples were stored under powdered dry ice in −80 °C freezers.

The extent of deuteration was determined by quickly thawing the frozen samples over melting ice and passing the solution through two immobilized protease columns (pepsin and fungal protease XIII from Sigma, 100 μl/min, 0.05% TFA). Peptides were separated by reverse-phase high pressure liquid chromatography (HPLC) (Vydac C-18 300A, 50 μl/min with a 6.4–38.4% acetonitrile gradient over 30 min, 4 °C). The effluent was directly injected into a mass spectrometer (ThermoFinnigan LCQ, capillary temperature of 200 °C). Initial identification of proteolytic fragments was determined by tandem MS followed by data analysis using the SEQUEST and DXMS software programs (ThermoFinnigan, San Jose, CA, and Sierra Analytics, Modesto, CA, respectively) (46, 47). Peptide deuteration levels were extracted from the centroid of individual mass envelopes according to the method of Zhang and Smith (48) after accounting for end effects and proline residues (29). Peptide deuteration levels were corrected for back exchange during proteolysis and chromatography based on their retention time in the chromatography step. Back exchange at the beginning of chromatography was found to be 15 and 20% at the end according to fully deuterated reference protein samples.

Cloning, Expression, and Purification—A synthetic gene for PrP(89–143, P101L) with an N-terminal six residue histidine tag and tobacco etch virus cleavage site was designed based on *Escherichia coli* optimum codon usage and synthesized by GenScript (Piscataway, NJ) in a pUC19 plasmid. This gene was subcloned into the pIVEX 2.4c vector between the NdeI and BamHI sites.

E. coli cells (BL21 (DE3)) containing a plasmid, pACYC, that constitutively expresses LacI were transformed using the hexamine cobalt chloride method (49) and grown on MDG (50) agar plates (1.5%) containing ampicillin and kanamycin at 37 °C for 12 h. A single colony was then picked and inoculated into 2 ml of MDAG media (100 μg/ml ampicillin, 50 μg/ml kanamycin) (50) and allowed to grow at 37 °C for 6 h. To obtain ^{15}N-labeled protein, 1 ml of this starter culture was used to inoculate 1 liter of N-5052 media (50) contained in a 2.8-liter Fernbach flask. Cells were allowed to grow for 48 h at 37 °C with shaking at 240 rpm. Cells expressing ^{13}C,^{15}N-labeled protein were obtained according to the method of Marley *et al.* (51) with the substitution of MDAG media for LB.

The cells were recovered by centrifugation at 5,000 rpm for 10 min and resuspended in ~40 ml of 50 mM KP_i, pH 8.0, and lysed by sonication at 4 °C. The resulting suspension was centrifuged for 30 min at 30,000 rpm. The supernatant was discarded, and the inclusion body was resolubilized by applying three rounds of resuspension in 6 M GdnHCl, 200 mM NaP_i, pH

8.0, 300 mM NaCl, 5 mM β-mercaptoethanol followed by centrifugation for 30 min at 30,000 rpm. The supernatants were pooled together and loaded onto nickel-nitrilotriacetic acid resin (6 ml). The column was then washed with a linear gradient from 6 to 0 M GdnHCl, 50 mM NaP_i, pH 8.0, 300 mM NaCl, and 15 mM imidazole. The protein was eluted from the column with 50 mM NaP_i, pH 8.0, 300 mM NaCl, and 500 mM imidazole and then dialyzed extensively against 50 mM Tris, pH 8.0, 1 mM DTT, 1 mM EDTA at 4 °C. One milligram of tobacco etch virus protease was added to the dialysis bag, and the cleavage reaction was monitored by HPLC. After complete proteolysis to remove the His tag, the solution was dialyzed against 50 mM NaP_i, pH 8.0, 300 mM NaCl, and 15 mM imidazole and then passed over nickel-nitrilotriacetic acid resin to remove both the His tag fragment and tobacco etch virus and desalted using a C18 Sep-Pak cartridge (Waters). The solution was frozen and lyophilized. Dry peptide was stored in a desiccator. On average, 15 mg of purified ^{15}N-labeled PrP(89–143, P101L) was obtained per 1 liter of growth. 0.5 mg of purified ^{13}C,^{15}N-labeled PrP(89–143, P101L) was obtained from 0.5 liter of M9 media.

NMR Experiments (Assignments)—All data were collected on a Bruker Avance DRX-500 or an Avance DRX-800 spectrometer equipped with a cryogenic probe, with samples kept at 25 °C. A single ^{15}N,^{13}C-labeled sample of PrP(89–143, P101L) consisting of 0.5 mg of protein dissolved in 500 μl of DMSO (5% H_2O, 0.03% TFA) was used for backbone assignments. Assignment of the ^{1}H,^{15}N HSQC spectrum was accomplished via inter-residue connection of the Cα, Cβ, and N chemical shifts using the HNCA, CBCA(CO)NH, and HNCACB experiments (52–54). Data were processed with NMRPipe (55). For the three-dimensional experiments, data were linear predicted to 128 pts in the ^{15}N dimension. Analysis and integration of data were performed with NMRView or CARA (56, 57).

Hydrogen Exchange NMR Spectroscopy—Fibrillization of ^{15}N-labeled PrP(89–143, P101L) was performed as outlined above. Approximately 0.5 mg of fibrillized ^{15}N-labeled PrP(89–143, P101L) was aliquoted into a separate Eppendorf tube for each exchange time point. Fibrils were resuspended in 10 mM KP_i, pD 7.5, and incubated at room temperature for varying periods of time. At the end of each time point, the fibrils were pelleted by centrifugation and washed twice with D_2O at 4 °C. After removing the supernatant, the fibrils were frozen over dry ice and lyophilized. Lyophilized fibrils were dissolved in DMSO containing 5% D_2O and 0.03% TFA-D, pH* 5. A series of ^{1}H,^{15}N HSQCs was collected over 8 h to correct for exchange with solvent under the quenching NMR sample conditions (32). The dead time from the addition of quenching/denaturing solvent to the fibrils to the acquisition of the first time point of the two-dimensional experiment was ~10 min (allowing for mixing to aid fibril dissolution and optimizing parameters for the NMR experiment). Each ^{1}H,^{15}N HSQC signal was the average of four transients, with 128 complex points acquired in the t_1 dimension, for a total acquisition time of 20 min per two-dimensional data set.

The intrinsic exchange rate in DMSO was determined by first integrating the volumes for each peak in each ^{1}H,^{15}N HSQC spectrum acquired over the 8 h. These individual volumes *versus* time were then plotted and fitted to single exponentials. The calculated rates from the exponential fits were then used to account for exchange during the dead time of the experiment. The intrinsic exchange rates are shown in supplemental Table S1. A 1–1-echo one-dimensional ^{1}H NMR spectrum was acquired for each sample, and the methyl region of the spectrum was integrated to normalize sample concentrations, which did not deviate by more than 3% between samples. Hydrogen exchange incubation times were 0, 1, 6, and 21 h and 1 and 6 weeks.

RESULTS

Hydrogen Exchange Mass Spectrometry of PrP(89–143, P101L) Fibrils—Synthetic PrP(89–143, P101L) fibrils that had been grown in H_2O were incubated in D_2O (buffered with sodium phosphate at pD 7.5) and aliquots removed after incubation for 1, 6, and 21 h and 1, 3, and 6 weeks. To determine the deuterium content of the fibrils using electrospray ionization mass spectrometry, the fibrils were redissolved by the addition of an aqueous buffer containing guanidine hydrochloride at low pH to quench hydrogen exchange, limiting back exchange during the mass analysis. To identify sites retaining deuterium in the primary sequence, exchange-quenched peptide solutions were fragmented using two protease columns containing immobilized pepsin and fungal protease XIII. Both proteases retain activity under quenching conditions. The peptide fragments were then separated by reverse-phase HPLC with the eluent running directly into the mass spectrometer. The ability to resolve slowly exchanging sites depends on the degree of fragmentation obtained, which in optimal circumstances can discriminate single amides. Peptides were identified in a reference experiment in which nondeuterated PrP(89–143, P101L) was proteolyzed in the same manner, and eluting fragments were then analyzed by tandem MS (58). Peptides in the deuterated samples were then identified by matching both mass and retention time.

Fig. 1 shows the extent of amide exchange of PrP(89–143, P101L) in fibrils after incubation in D_2O for 6 weeks observed using mass spectrometry. 34 "primary" peptide fragments were obtained with good signal to noise ratios in repeated experiments at each time point studied. Exchange in 23 additional "secondary" peptide segments could be analyzed via deuterium level subtraction of N-terminally aligned peptides of different length; N-terminal alignment of peptides is required to correct for end effects. Although PrP(89–143, P101L) was not proteolyzed sufficiently before mass spectrometry to afford single site resolution, a consensus exchange behavior can be approximated by calculating an average of the exchange behavior in which the contribution from each observed peptide is weighted according to the information content of the peptide. The longer the peptide, the less information for localization of exchange it contains. The averaging is performed according to Equation 1,

$$HX = \sum_{i=1}^{n}\left(\frac{hx_i}{\text{length}_i}\right) \Big/ \sum_{i=1}^{n}\frac{1}{\text{length}_i} \qquad \text{(Eq. 1)}$$

where HX is the averaged percent protection; hx_i is the percent

protection of each peptide *i*; *n* represents the number of peptides in which a given residue is observed, and length$_i$ is the length of each peptide *i*. Although the data do not afford single amide resolution, it is clear that there is a strongly protected region between residues 119 and 130, increased protection at the C terminus, and two regions from 99 to 107 and 133 to 139 that show significantly lower protection from exchange with solvent.

Recombinant Expression and Fibrillization of PrP(89–143, P101L)—Amide hydrogen exchange at individual sites can be detected with NMR, but it requires isotopically labeled protein. To obtain uniformly and isotopically labeled PrP(89–143, P101L) for heteronuclear NMR experiments, we developed an *E. coli* expression system in which purification of the peptide was expedited by the presence of an N-terminal His$_6$ tag. The supplemental Fig. S1 shows the results from a typical purification process and shows an electron micrograph of PrP(89–143, P101L) fibrils produced from recombinant peptide. Fibrils were grown with the same procedure used to fibrillize synthetic peptide that initiated prion disease in sensitized transgenic mice (43).

Sequence-specific Detection of Hydrogen Exchange in PrP(89–143, P101L) Fibrils—As in the mass spectrometry exchange experiments, detecting the extent of hydrogen exchange in amyloid fibrils with NMR requires the denaturation of fibrils under exchange quenching conditions prior to data collection. Acidic dimethyl sulfoxide (DMSO) is an excellent quench solvent to dissolve amyloid fibrils (31, 32, 34, 59, 60). The minimum rate for amide hydrogen exchange in DMSO occurs at pH* 5 and is typically on the order of 10^{-5} s^{-1} (61). All non-proline residues have been assigned for the 55-mer with the exception of the N-terminal glycine that exchanges too quickly to be observed in the NMR experiment and four ambiguous glycine resi-

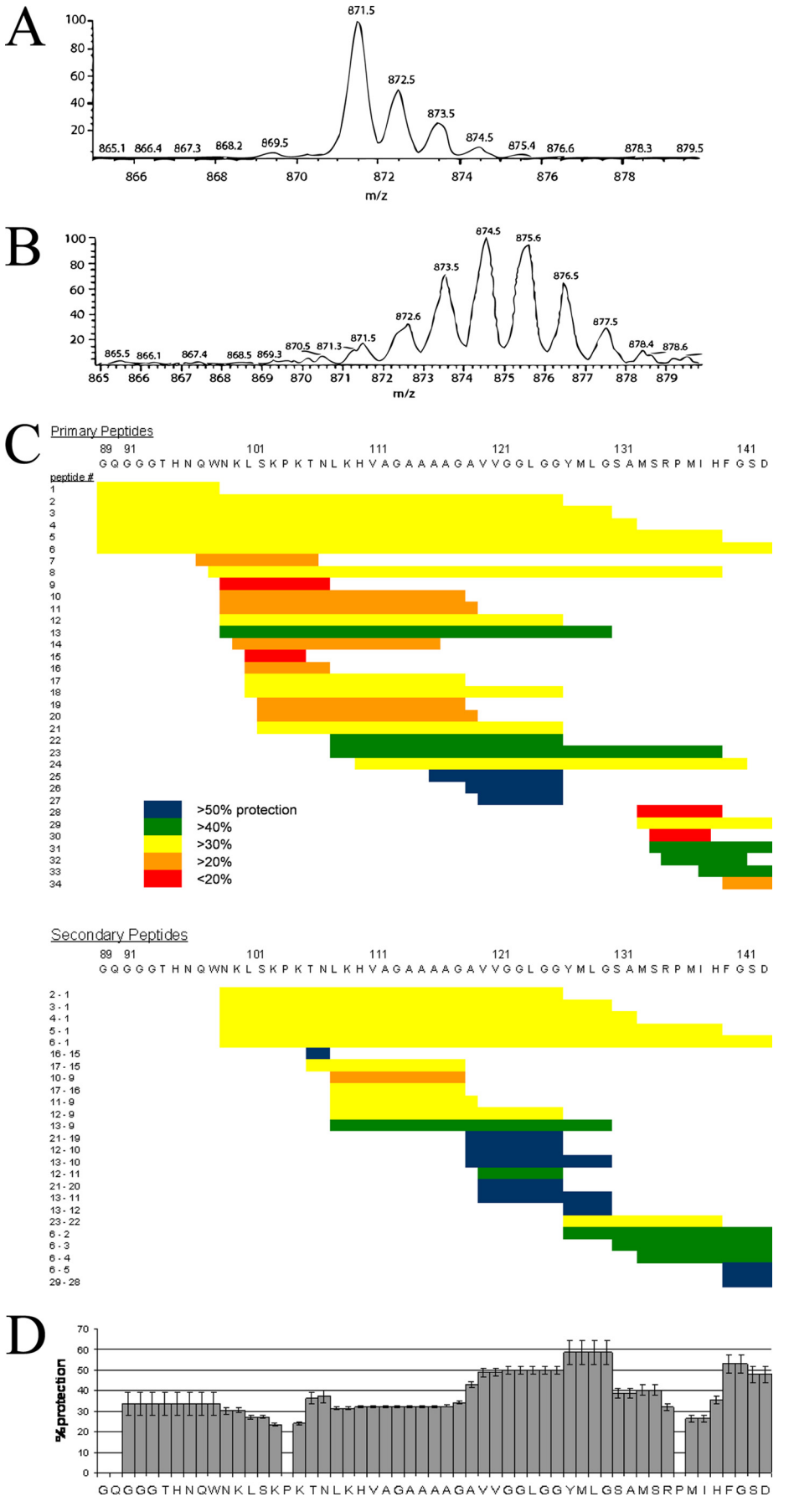

dues that occur in glycine-glycine pairs in the sequence. These residues have very similar exchange behavior; therefore, it is not important to individually assign them.

Dissolution of the fibrils and optimization of the NMR experiment lead to a "dead time" of approximately 10 min for each sample before NMR data collection. Because the DMSO contains a small amount of D_2O, multiple $^1H,^{15}N$ HSQC spectra were collected over a period of 6–8 h after dissolving for each exchange time point to determine the intrinsic rate of exchange in DMSO for each amide. This allows one to discriminate between the exchange that occurs during the incubation of the fibrils in deuterated buffer and the exchange that occurs during the dead time for handling the sample. The intrinsic rate of amide exchange under quenching NMR conditions was slow for all residues as confirmed by exchange measurements on fibrils that had not been exposed to deuterated buffers. The measured rate of exchange for all residues was on the order of 10^{-5} s^{-1} (data not shown), which corresponds to a half-life of hours, so that little exchange occurs during the measurement time of the experiment.

Given the small number of time points in the experimental data set and the limited range of time sampled, the slow exchange rates of the backbone cannot be quantified with certainty. Therefore, we present the exchange data using a percent intensity (I_P) given by Equation 2,

$$I_R = I_t/I_0 \times 100\% \qquad \text{(Eq. 2)}$$

where I_t is the integrated intensity (corrected for back exchange and normalized by concentration) for a given amide cross-peak at time t, and I_0 is the integrated intensity (corrected for back exchange and normalized by concentration) for the 0-h time point. The calculated I_P values for each residue for each experimental time point are shown in Table 1. Four types of exchange behavior were observed and are summarized in Fig. 2. The amide hydrogens of residues 90 and 143, the terminal amides, exchange completely before the first time point. Residues 95–101 and 137–141 exchange more slowly, with a half-life of approximately a week, but are completely replaced after 6 weeks. Residues 110–116 exchange slowly as well, with similar extents of exchange after a week as residues 95–101, but retain $I_P \sim 50$ even after 6 weeks, which implies a multiexponential behavior in the rates. Finally, residues 102–109 and 117–135 remain highly protected even after 6 weeks ($I_P > 90$).

TABLE 1

Percent intensity (see Equation 2)

A listing of measured I_P (Equation 2) values for each residue of PrP(89–143, P101L) amyloid fibrils from the hydrogen exchange experiment. The exchange behavior of the four ambiguous glycine residues (marked by an asterisk) is reported as an average, the exchange behavior of each was similar.

Residue	0-hour	1-hour	6-hour	21-hour	1 week	6 weeks
G89	-					
Q90	100	0	0	0	0	0
G91	100	103	0	0	0	0
G92*	100	99	96	89	89	80
G93*	100	99	96	89	89	80
T94	100	87	93	85	87	75
H95	100	86	80	75	38	0
N96	100	89	89	82	68	3
Q97	100	93	82	80	59	0
W98	100	95	94	80	52	0
N99	100	95	96	79	54	0
K100	100	100	99	83	55	0
L101	100	108	99	90	61	6
S102	100	100	99	93	90	80
K103	100	92	97	80	86	85
P104	-					
K105	100	100	100	87	82	79
T106	100	99	99	99	96	88
N107	100	97	99	92	80	84
L108	100	92	96	93	93	90
K109	100	100	102	99	90	79
H110	100	93	99	82	50	52
V111	100	82	90	90	44	38
A112	100	91	88	93	49	43
G113	100	100	92	87	58	53
A114	100	95	101	90	47	41
A115	100	100	95	97	50	30
A116	100	99	104	95	60	58
A117	100	101	99	88	85	80
G118	100	99	90	93	89	87
A119	100	100	103	95	90	90
V120	100	96	101	85	90	88
V121	100	92	92	86	90	82
G122	100	103	92	90	90	83
G123*	100	99	96	89	89	80
L124	100	100	85	95	90	95
G125	100	103	90	89	90	83
G126*	100	99	96	89	89	80
Y127	100	100	93	81	77	72
M128	100	89	85	80	80	65
L129	100	92	90	86	81	69
G130	100	100	99	94	89	81
S131	100	93	93	89	80	76
A132	100	99	100	90	90	88
M133	100	88	93	82	91	86
S134	100	99	94	92	84	82
R135	100	99	88	87	75	81
P136	-					
M137	100	97	94	90	56	0
L138	100	100	100	89	60	2
H139	100	97	93	95	49	0
F140	100	98	92	88	59	4
G141	100	103	100	85	43	0
S142	100	92	92	83	84	78
D143	100	0	0	0	0	0

DISCUSSION

Previous solid-state NMR studies of selectively and isotopically labeled PrP(89–143, P101L) fibrils from our laboratory have demonstrated that residues 112–124 adopt an extended β-sheet conformation with evidence for conformational heterogeneity between residues 112 and 114. Furthermore, multiple quantum NMR experiments indicated that PrP(89–143, P101L) does not adopt an in-register parallel β-sheet (62). To extend our knowledge of the conformation of fibrillar PrP(89–143, P101L), we measured the extent of backbone hydrogen exchange at various time points up to 6 weeks of exchange. In the most favorable cases, following hydrogen exchange with

FIGURE 1. **Exchange behavior of PrP(89–143, P101L) fibrils observed by mass spectrometry.** *A*, shows the mass envelope of the 1+ charge state of the proteolytic fragment of PrP(89–143, P101L) corresponding to residues 133–139. *B*, mass envelope of the same peptide obtained from PrP fibrils that had been incubated in D_2O for 1 week. *C*, exchange behavior of proteolytic fragments of PrP(89–143, P101L) after 6 weeks of incubation in D_2O. The extent of exchange is depicted as a percent protection of exchangeable backbone amides. Each primary peptide is numbered. The identity of the two primary peptides used to obtain each secondary peptide is indicated to the *left* of the secondary peptides. *D*, consensus exchange behavior calculated according to Equation 1.

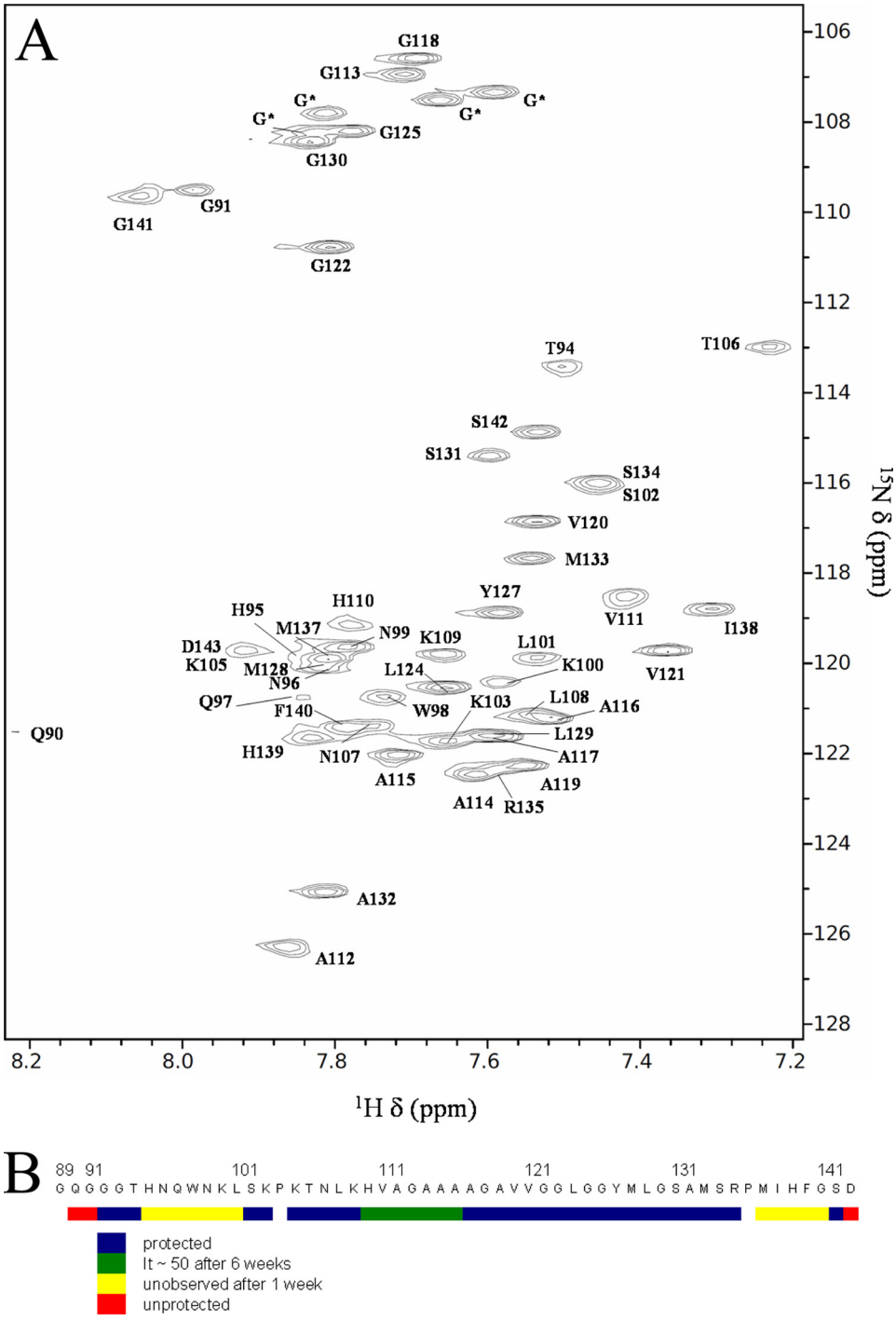

FIGURE 2. **Exchange behavior of PrP(89–143, P101L) fibrils observed with NMR.** *A*, shows the assigned ^{1}H,^{15}N HSQC spectrum of PrP(89–143, P101L) under the conditions of a typical 0-h time point, dissolving fibrils that had not been exposed to deuterium in DMSO containing 5% D_2O and 0.03% TFA-D, pH* 5. The four ambiguous glycine residues are denoted with an *asterisk*. *B,* summary of the exchange behavior of PrP(89–143, P101L) fibrils.

In our MS study of exchange in fibrillar PrP(89–143, P101L), the limited number of peptide fragments observed with sufficient signal to noise for analysis precluded single amide resolution of exchange behavior. However, the data from mass spectrometry clearly demonstrate that there are regions of the peptide that are strongly protected from exchange with solvent, whereas other regions are much less protected from exchange. This is expected as the 55-residue peptide is too long to exist as a single, stably hydrogen-bonded, extended strand within the fibril as the fibril diameter is known to be ~8 nm. The exchange profile reveals a highly protected β-strand region with residues 119–130, flanked by two segments that are within a less protected region, encompassing residues 99–107 and 133–139. Fragmentation was poor near the N terminus preventing analysis of that region.

To generate a higher resolution map of protection, more detailed exchange data were required. After assigning the resonances of PrP(89–143, P101L), we collected amide exchange profiles by following exchange with NMR. Many of the residues show the slow exchange behavior expected from amides involved in stable hydrogen bonds. Two regions, encompassing residues 102–109 and 117–135, remained protected from exchange after 6 weeks and likely constitute the β-sheet core of the fibrils. The high degree of protection is not surprising in that some residues in β_2-microglobulin amyloid have been shown to have exchange half-lives of weeks (39) and some residues in Aβ amyloid have been shown to have half-lives of months (33, 34). Another set of residues, close to the N terminus and at the C terminus, were completely exchanged after 6 weeks of incubation in D_2O. Although residues 95–101 and 137–141 have moderate protection factors that are typically afforded by secondary structure conformations in soluble proteins, they exchange more rapidly than the β-sheet core residues of other reported amyloid fibrils. The lower protection in these two regions is consistent with the mass spectrometry measurements.

tandem proteolysis and LC-MS (HXMS) can lead to single amide resolution. Moreover, HXMS is ideally suited to study prions as it does not require isotopically labeled samples; thus, it is one of the few techniques suited to studying the conformation of PrP^{Sc} obtained directly from infected animals. The exchange behavior of natural PrP^{Sc} could then be compared with that of different constructs of recombinant or synthetic PrP, which are much more tractable to analysis.

Interestingly, residues 110–116 show exchange behavior characteristic of multiple exponentials. This group of residues undergoes exchange to ~50% after 1 week. However, after 6 weeks, no further exchange has occurred. This behavior can be explained by the presence of two (or more) conformations for these residues present in the sample with different exchange rates. One component has a half-life of approximately 1 week, and the second component has a much longer half-life. The mass spectrometry data in this region are also consistent with intermediate protection, but we lack sufficient sequence resolution to observe a bimodal deuterium distribution for this region of the peptide that would confirm the presence of two populations of conformers, one more accessible to exchange with solvent than the other. Furthermore, the residues 110–116 encompass the region of the peptide that displayed conformational heterogeneity in past solid-state NMR experiments (62). It is possible that different conformers could give rise to prion strains observed *in vivo* (63).

Currently, there are several different models for the conformation of PrP in prions (64). One is a left-handed β-helix proposed by Govaerts *et al.* (24) from two-dimensional electron crystallography data on proteolyzed native PrP^{Sc}. Another is a "spiral" model identified in a molecular dynamics study of PrP fibrillization that was also shown to be consistent with the electron crystallography data (27). Neither the β-helix nor the spiral model requires the fibril to be formed by an in-register parallel β-sheet as seen in Aβ fibrils (34), consistent with previous observations from solid-state NMR (62). A solid-state NMR study on fibrils of another prion variant, human PrP(Y145Stop), has demonstrated that the N terminus of the protein, up to residue 112, remains highly mobile in the fibril and that residues 112–115, 118–122, and 130–139 form β-strands (65); the corresponding regions in the mouse protein are residues 111–114, 117–121, and 129–138. Another recent structural model has been obtained from HXMS experiments conducted on prion fibrils of PrP(89–230), in that work protection from exchange is only observed in the C-terminal region of the protein, approximately residues 168–220 (3, 40). This in disagreement with the previously discussed structural models and also lies outside of the region of interest studied in this work (residues 89–143). As the Y145Stop variant has been identified in human prion disease, the prion determining region of PrP cannot be wholly contained to the C terminus of the protein (66, 67). Moreover, it is well documented that different strains of prions can assume drastically different conformations. For example, the highly protected core of Sup35 yeast prions consists of ~40 residues in one strain and ~70 residues in a different strain (68). Finally, the protease-resistant PrP present in patients with GSS contains a significant amount of 7–8-kDa PrP fragments. These fragments possess ragged N termini beginning around residue 80 and also ragged C termini ending around residue 150, encompassing the region of interest in this study (69, 70). Furthermore, it has been shown that the synthetic prions used in the HXMS study by Lu *et al.* (40, 71) are more susceptible to degradation by proteinase K than "classical" PrP^{Sc} and are similar to a subpopulation of PrP^{Sc}, recently identified in patients, rather than the classical PrP^{Sc}. In fact, further HXMS experiments from the Surewicz laboratory demonstrate that PrP^{Sc}-seeded recombinant PrP aggregates are significantly more protected from exchange than the spontaneously aggregated proteins studied by Lu *et al.* (40, 71). Also, similarly to PrP(89–143, P101L) fibrils, the PrP^{Sc}-seeded aggregates contain a protected region between residues 116 and 132 (72). For the reasons outlined above, we argue that the precise location of the fibrillar core in prion aggregates varies significantly based on both the prion strain, the particular PrP construct employed, and the conditions under which the peptide is aggregated.

In the β-helical model, three 5-residue strands are joined by a single residue that has torsion angles characteristic of a left-handed helix to form a triangular 18-residue "rung," and these rungs are then stacked in a stably hydrogen-bonded network, including a hydrogen bond at each residue, to form the β-helix. Our exchange data show that the region from 102 to 136 is resistant to exchange with some degree of conformational heterogeneity from 110 to 116. This span of the peptide is essentially long enough to support two rungs of a β-helix, but PrP(89–143, P101L) is rather unlikely to adopt this conformation as in nature the minimal number of "rungs" found experimentally to date is four (seen in the structure of the C-terminal domain of *N*-acetylglucosamine-1-phosphate uridyltransferase from *E. coli*, Protein Data Bank code 1FXJ). However, in the fibril, monomers could be packing against each other to extend the helix. More difficult to reconcile than the length issue is the fact that the previous solid-state NMR experiments on PrP(89–143, P101L) did not find any evidence of turn conformations between residues 112 and 118 and between residues 122 and 124 (62). If the core of the fibril is formed by a β-helix, some of these residues should be clearly involved in turns.

The core of the spiral model of PrP^{Sc} consists of four short β-strands in which three short strands (E1, E2, E3; residues 115–118, 128–131, 159–163, respectively) form an anti-parallel intramolecular sheet where the extra strand (E4, residues 134–139) adds to the sheet on an adjacent molecule through a parallel E1-E4 interface. E3 is not essential for the formation of the intermolecular interface; however, the positions of the protected residues in PrP(89–143, P101L) fibrils are not consistent with the location of E1, E2, and E4 in the model, although the spiral architecture could explain the protection factors and the observation that PrP(89–143, P101L) fibrils do not form an in-register β-sheet.

In summary, our hydrogen exchange experiments identify two regions of the protein, encompassing residues 102–109 and 117–135, that display strong protection from exchange with solvent even after 6 weeks and are likely to constitute the core of the fibril. Two other regions, encompassing residues 95–101 and 137–141, exchange completely with solvent after 1 week, an exchange time expected for residues involved in hydrogen bonds but not in the amyloid core. Interestingly, the region of the protein between residues 110 and 116 exhibits intermediate exchange behavior that can be explained by the existence of two populations of conformers in the fibril that exchange with solvent at different rates. This interpretation of the intermediate protection factors is corroborated by our previous finding that this region possesses some conformational heterogeneity (62). The core of the PrP(89–43, P101L) amyloid fibril consists of

two highly protected β-strands (β1 and β2, residues 102–109 and 117–136, respectively) that are joined by a hydrogen-bonded yet conformationally heterogeneous turn. The overall fibril architecture must be different from that seen in fibrils of Aβ as the PrP fibrils have been shown to not be in register. Assuming slightly different locations of strands E1, E2, and E4 from the spiral model, the core of the fibril could form from an intramolecular sheet between β1 and the first section of β2 where the intermolecular interface is between the second section of β2 and β1 on the adjacent molecule. Finally, we stress that HXMS is one of the few techniques that can assess the conformation of natural prions and will be extremely valuable in comparing synthetic prions to those obtained directly from infected animals.

Acknowledgments—We thank Prof. Stan Prusiner and co-workers for discussions about prion behavior and Dr. David King for the synthesis of PrP(89-143, P101L).

REFERENCES

1. DeArmond, S. J., and Prusiner, S. B. (1996) *Current Topics in Microbiology and Immunology* (Prusiner, S. B., ed) Vol. 207, pp. 125–146, Springer, New York
2. Prusiner, S. B. (2004) in *Prion Biology and Diseases* (Prusiner, S. B., ed) pp. 89–141, Cold Spring Harbor Laboratory Press, Cold Spring Harbor, NY
3. Legname, G., Baskakov, I. V., Nguyen, H. O., Riesner, D., Cohen, F. E., DeArmond, S. J., and Prusiner, S. B. (2004) *Science* **305,** 673–676
4. Wang, F., Wang, X., Yuan, C. G., and Ma, J. (2010) *Science* **327,** 1132–1135
5. Deleault, N. R., Harris, B. T., Rees, J. R., and Supattapone, S. (2007) *Proc. Natl. Acad. Sci. U.S.A.* **104,** 9741–9746
6. Deleault, N. R., Geoghegan, J. C., Nishina, K., Kascsak, R., Williamson, R. A., and Supattapone, S. (2005) *J. Biol. Chem.* **280,** 26873–26879
7. Geoghegan, J. C., Valdes, P. A., Orem, N. R., Deleault, N. R., Williamson, R. A., Harris, B. T., and Supattapone, S. (2007) *J. Biol. Chem.* **282,** 36341–36353
8. Baron, G. S., Magalhães, A. C., Prado, M. A., and Caughey, B. (2006) *J. Virol.* **80,** 2106–2117
9. Gabizon, R., McKinley, M. P., and Prusiner, S. B. (1987) *Proc. Natl. Acad. Sci. U.S.A.* **84,** 4017–4021
10. Silva, J. L., Lima, L. M., Foguel, D., and Cordeiro, Y. (2008) *Trends Biochem. Sci.* **33,** 132–140
11. Lima, L. M., Cordeiro, Y., Tinoco, L. W., Marques, A. F., Oliveira, C. L., Sampath, S., Kodali, R., Choi, G., Foguel, D., Torriani, I., Caughey, B., and Silva, J. L. (2006) *Biochemistry* **45,** 9180–9187
12. Lysek, D. A., Schorn, C., Nivon, L. G., Esteve-Moya, V., Christen, B., Calzolai, L., von Schroetter, C., Fiorito, F., Herrmann, T., Güntert, P., and Wüthrich, K. (2005) *Proc. Natl. Acad. Sci. U.S.A.* **102,** 640–645
13. Calzolai, L., Lysek, D. A., Pérez, D. R., Güntert, P., and Wüthrich, K. (2005) *Proc. Natl. Acad. Sci. U.S.A.* **102,** 651–655
14. Gossert, A. D., Bonjour, S., Lysek, D. A., Fiorito, F., and Wüthrich, K. (2005) *Proc. Natl. Acad. Sci. U.S.A.* **102,** 646–650
15. James, T. L., Liu, H., Ulyanov, N. B., Farr-Jones, S., Zhang, H., Donne, D. G., Kaneko, K., Groth, D., Mehlhorn, I., Prusiner, S. B., and Cohen, F. E. (1997) *Proc. Natl. Acad. Sci. U.S.A.* **94,** 10086–10091
16. Hornemann, S., Schorn, C., and Wüthrich, K. (2004) *EMBO Rep.* **5,** 1159–1164
17. Riek, R., Hornemann, S., Wider, G., Billeter, M., Glockshuber, R., and Wüthrich, K. (1996) *Nature* **382,** 180–182
18. Brown, D. R. (2003) *J. Neurochem.* **87,** 377–385
19. Garnett, A. P., and Viles, J. H. (2003) *J. Biol. Chem.* **278,** 6795–6802
20. Sakudo, A., Lee, D. C., Yoshimura, E., Nagasaka, S., Nitta, K., Saeki, K., Matsumoto, Y., Lehmann, S., Itohara, S., Sakaguchi, S., and Onodera, T. (2004) *Biochem. Biophys. Res. Commun.* **313,** 850–855
21. Aguzzi, A., Baumann, F., and Bremer, J. (2008) *Annu. Rev. Neurosci.* **31,** 439–477
22. Pan, K. M., Baldwin, M., Nguyen, J., Gasset, M., Serban, A., Groth, D., Mehlhorn, I., Huang, Z., Fletterick, R. J., Cohen, F. E., and Prusiner, S. B. (1993) *Proc. Natl. Acad. Sci. U.S.A.* **90,** 10962–10966
23. Prusiner, S. B., McKinley, M. P., Bowman, K. A., Bolton, D. C., Bendheim, P. E., Groth, D. F., and Glenner, G. G. (1983) *Cell* **35,** 349–358
24. Govaerts, C., Wille, H., Prusiner, S. B., and Cohen, F. E. (2004) *Proc. Natl. Acad. Sci. U.S.A.* **101,** 8342–8347
25. Wille, H., Michelitsch, M. D., Guenebaut, V., Supattapone, S., Serban, A., Cohen, F. E., Agard, D. A., and Prusiner, S. B. (2002) *Proc. Natl. Acad. Sci. U.S.A.* **99,** 3563–3568
26. DeMarco, M. L., Silveira, J., Caughey, B., and Daggett, V. (2006) *Biochemistry* **45,** 15573–15582
27. DeMarco, M. L., and Daggett, V. (2004) *Proc. Natl. Acad. Sci. U.S.A.* **101,** 2293–2298
28. Englander, S. W., Mayne, L., Bai, Y., and Sosnick, T. R. (1997) *Protein Sci.* **6,** 1101–1109
29. Bai, Y., Milne, J. S., Mayne, L., and Englander, S. W. (1993) *Proteins Struct. Funct. Genet.* **17,** 75–86
30. Del Mar, C., Greenbaum, E. A., Mayne, L., Englander, S. W., and Woods, V. L., Jr. (2005) *Proc. Natl. Acad. Sci. U.S.A.* **102,** 15477–15482
31. Hoshino, M., Katou, H., Hagihara, Y., Hasegawa, K., Naiki, H., and Goto, Y. (2002) *Nat. Struct. Biol.* **9,** 332–336
32. Ippel, J. H., Olofsson, A., Schleucher, J., Lundgren, E., and Wijmenga, S. S. (2002) *Proc. Natl. Acad. Sci. U.S.A.* **99,** 8648–8653
33. Kheterpal, I., Zhou, S., Cook, K. D., and Wetzel, R. (2000) *Proc. Natl. Acad. Sci. U.S.A.* **97,** 13597–13601
34. Lührs, T., Ritter, C., Adrian, M., Riek-Loher, D., Bohrmann, B., Döbeli, H., Schubert, D., and Riek, R. (2005) *Proc. Natl. Acad. Sci. U.S.A.* **102,** 17342–17347
35. Nazabal, A., Maddelein, M. L., Bonneu, M., Saupe, S. J., and Schmitter, J. M. (2005) *J. Biol. Chem.* **280,** 13220–13228
36. Olofsson, A., Ippel, J. H., Wijmenga, S. S., Lundgren, E., and Ohman, A. (2004) *J. Biol. Chem.* **279,** 5699–5707
37. Olofsson, A., Sauer-Eriksson, A. E., and Ohman, A. (2006) *J. Biol. Chem.* **281,** 477–483
38. Wang, S. S., Tobler, S. A., Good, T. A., and Fernandez, E. J. (2003) *Biochemistry* **42,** 9507–9514
39. Yamaguchi, K., Katou, H., Hoshino, M., Hasegawa, K., Naiki, H., and Goto, Y. (2004) *J. Mol. Biol.* **338,** 559–571
40. Lu, X., Wintrode, P. L., and Surewicz, W. K. (2007) *Proc. Natl. Acad. Sci. U.S.A.* **104,** 1510–1515
41. Hsiao, K. K., Scott, M., Foster, D., Groth, D. F., DeArmond, S. J., and Prusiner, S. B. (1990) *Science* **250,** 1587–1590
42. Hsiao, K. K., Groth, D., Scott, M., Yang, S. L., Serban, H., Rapp, D., Foster, D., Torchia, M., Dearmond, S. J., and Prusiner, S. B. (1994) *Proc. Natl. Acad. Sci. U.S.A.* **91,** 9126–9130
43. Kaneko, K., Ball, H. L., Wille, H., Zhang, H., Groth, D., Torchia, M., Tremblay, P., Safar, J., Prusiner, S. B., DeArmond, S. J., Baldwin, M. A., and Cohen, F. E. (2000) *J. Mol. Biol.* **295,** 997–1007
44. Tremblay, P., Ball, H. L., Kaneko, K., Groth, D., Hegde, R. S., Cohen, F. E., DeArmond, S. J., Prusiner, S. B., and Safar, J. G. (2004) *J. Virol.* **78,** 2088–2099
45. Woods, V. L., Jr., and Hamuro, Y. (2001) *J. Cell. Biochem. Suppl.* **37,** 89–98
46. Pantazatos, D., Kim, J. S., Klock, H. E., Stevens, R. C., Wilson, I. A., Lesley, S. A., and Woods, V. L., Jr. (2004) *Proc. Natl. Acad. Sci. U.S.A.* **101,** 751–756
47. Englander, J. J., Del Mar, C., Li, W., Englander, S. W., Kim, J. S., Stranz, D. D., Hamuro, Y., and Woods, V. L., Jr. (2003) *Proc. Natl. Acad. Sci. U.S.A.* **100,** 7057–7062
48. Zhang, Z., and Smith, D. L. (1993) *Protein Sci.* **2,** 522–531
49. Hanahan, D. (1983) *J. Mol. Biol.* **166,** 557–580
50. Studier, F. W. (2005) *Protein Expr. Purif.* **41,** 207–234
51. Marley, J., Lu, M., and Bracken, C. (2001) *J. Biomol. NMR* **20,** 71–75
52. Grzesiek, S., and Bax, A. (1992) *J. Magn. Res.* **96,** 432–440
53. Grzesiek, S., and Bax, A. (1993) *J. Biomol. NMR* **3,** 185–204
54. Wittekind, M., and Mueller, L. (1993) *J. Magn. Res.* **B101,** 201–205
55. Delaglio, F., Grzesiek, S., Vuister, G. W., Zhu, G., Pfeifer, J., and Bax, A.

(1995) *J. Biomol. NMR* **6,** 277–293
56. Johnson, B. A., and Blevins, R. A. (1994) *J. Biomol. NMR* **4,** 603–614
57. Keller, R. (2004) *The Computer Aided Resonance Assignment Tutorial*, Cantina Verlag, Goldau, Switzerland
58. Eng, J. K., McCormack, A. L., and Yates, J. R. (1994) *J. Am. Soc. Mass Spectrom.* **5,** 976–989
59. Hirota-Nakaoka, N., Hasegawa, K., Naiki, H., and Goto, Y. (2003) *J. Biochem.* **134,** 159–164
60. Ritter, C., Maddelein, M. L., Siemer, A. B., Lührs, T., Ernst, M., Meier, B. H., Saupe, S. J., and Riek, R. (2005) *Nature* **435,** 844–848
61. Zhang, Y. Z., Paterson, Y., and Roder, H. (1995) *Protein Sci.* **4,** 804–814
62. Lim, K. H., Nguyen, T. N., Damo, S. M., Mazur, T., Ball, H. L., Prusiner, S. B., Pines, A., and Wemmer, D. E. (2006) *Solid State Nuclear Magnetic Resonance* **29,** 183–190
63. Legname, G., Nguyen, H. O., Baskakov, I. V., Cohen, F. E., Dearmond, S. J., and Prusiner, S. B. (2005) *Proc. Natl. Acad. Sci. U.S.A.* **102,** 2168–2173
64. Cobb, N. J., and Surewicz, W. K. (2009) *Biochemistry* **48,** 2574–2585
65. Helmus, J. J., Surewicz, K., Nadaud, P. S., Surewicz, W. K., and Jaroniec, C. P. (2008) *Proc. Natl. Acad. Sci. U.S.A.* **105,** 6284–6289
66. Ghetti, B., Piccardo, P., Spillantini, M. G., Ichimiya, Y., Porro, M., Perini, F., Kitamoto, T., Tateishi, J., Seiler, C., Frangione, B., Bugiani, O., Giaccone, G., Prelli, F., Goedert, M., Dlouhy, S. R., and Tagliavini, F. (1996) *Proc. Natl. Acad. Sci. U.S.A.* **93,** 744–748
67. Kundu, B., Maiti, N. R., Jones, E. M., Surewicz, K. A., Vanik, D. L., and Surewicz, W. K. (2003) *Proc. Natl. Acad. Sci. U.S.A.* **100,** 12069–12074
68. Toyama, B. H., Kelly, M. J., Gross, J. D., and Weissman, J. S. (2007) *Nature* **449,** 233–237
69. Parchi, P., Chen, S. G., Brown, P., Zou, W., Capellari, S., Budka, H., Hainfellner, J., Reyes, P. F., Golden, G. T., Hauw, J. J., Gajdusek, D. C., and Gambetti, P. (1998) *Proc. Natl. Acad. Sci. U.S.A.* **95,** 8322–8327
70. Piccardo, P., Liepnieks, J. J., William, A., Dlouhy, S. R., Farlow, M. R., Young, K., Nochlin, D., Bird, T. D., Nixon, R. R., Ball, M. J., DeCarli, C., Bugiani, O., Tagliavini, F., Benson, M. D., and Ghetti, B. (2001) *Am. J. Pathol.* **158,** 2201–2207
71. Bocharova, O. V., Breydo, L., Salnikov, V. V., Gill, A. C., and Baskakov, I. V. (2005) *Protein Sci.* **14,** 1222–1232
72. Smirnovas, V., Kim, J. I., Lu, X., Atarashi, R., Caughey, B., and Surewicz, W. K. (2009) *J. Biol. Chem.* **284,** 24233–24241